Effective construction of divergence-free wavelets on the square

Souleymane Kadri Harouna, Valérie Perrier

Effective construction of divergence-free wavelets on the square

S. Kadri Harouna[a], V. Perrier[b]

[a] *INRIA Rennes - Bretagne Atlantique, Campus Universitaire de Beaulieu, 35042 Rennes cedex, France*
[b] *Laboratoire Jean Kuntzmann, Université de Grenoble et CNRS UMR 5224, B.P. 53, 38401 Grenoble cedex 9, France*

Abstract

We present an effective construction of divergence-free wavelets on the square, with suitable boundary conditions. Since 2D divergence-free vector functions are the curl of scalar stream-functions, we simply derive divergence-free multiresolution spaces and wavelets by considering the curl of standard biorthogonal multiresolution analyses (BMRAs) on the square. The key point of the theory is that the derivative of a 1D BMRA is also a BMRA, as established by Jouini and Lemarié-Rieusset [11]. We propose such construction in the context of generic compactly supported wavelets, which allows fast algorithms. Examples illustrate the practicality of the method.

Keywords: Divergence-free wavelets, biorthogonal multiresolution analyses, Dirichlet boundary conditions

1. Introduction

Divergence-free wavelets on the whole space $\mathbb{R}^d$ have been firstly constructed by Battle-Federbush in the orthogonal case [3], and by Lemarié-Rieusset in the biorthogonal one [15]. A first implementation for the analysis of incompressible vector fields was carried out by Urban [20]. More recently, Deriaz-Perrier propose an alternative fast decomposition into divergence-free wavelets based on anisotropic (tensor-product) wavelets in the periodic case [7]. First extensions of these constructions to the hypercube $\Omega = [0,1]^d$ were published by Stevenson in [18, 19]. In particular [19] addresses the problem of finding bases of the divergence-free vector space, with free-slip boundary conditions:

$$\mathcal{H}_{div}(\Omega) = \{\mathbf{u} \in (L^2(\Omega))^d : \ \mathbf{div}(\mathbf{u}) = 0 \text{ and } \mathbf{u} \cdot \vec{\nu} = 0\}. \tag{1}$$

This space occurs in the resolution of incompressible Navier-Stokes equations in velocity-pressure formulation with Dirichlet boundary conditions for the velocity

Email addresses: souleymane.kadri_harouna@inria.fr (S. Kadri Harouna), Valerie.Perrier@imag.fr (V. Perrier)

at the boundary [9]. Having at hand a divergence-free basis and associated finite-dimensional approximation vector spaces of $\mathcal{H}_{div}(\Omega)$ is the key-point for developing new numerical methods for the direct simulation of turbulence, as proposed in [8] in the periodic case.

Our objective in the present paper is to propose, in the two-dimensional case, an alternative construction to [19] of wavelet bases of $\mathcal{H}_{div}(\Omega)$, more generic and effective. Indeed, unlike the construction [19], our bases follow from standard biorthogonal wavelets on the interval satisfying homogeneous boundary conditions, which include a wide variety of functions and will provide fast divergence-free wavelet decompositions. Our construction is based on two arguments:

Firstly in the 2D case, the space $\mathcal{H}_{div}(\Omega)$ coincides with the curl of scalar stream functions with vanishing boundary conditions [9]:

$$\mathcal{H}_{div}(\Omega) = \{\mathbf{u} = \mathbf{curl}\ \chi\ ;\ \chi \in H_0^1(\Omega)\}. \tag{2}$$

Moreover in the simple case of a square domain, the curl is an isomorphism from $H_0^1(\Omega)$ to $\mathcal{H}_{div}(\Omega)$ [9], then wavelet bases can be simply constructed by taking the curl of scalar wavelet bases of $H_0^1(\Omega)$. The most common way to construct such bases of $H_0^1(\Omega)$ is to consider tensor products of one-dimensional wavelets of $H_0^1(0,1)$: these 1D wavelets arise from 1D multiresolution analyses of $H^1(0,1)$, (V_j^1), as constructed in a significant number of works [5, 6, 10], and adapted to homogeneous boundary conditions by skipping one function at each boundary [4, 16, 17].

The second argument in our construction follows from the work of Jouini - Lemarié-Rieusset [11], which states that the derivative spaces $\frac{d}{dx}V_j^1 = V_j^0$ constitute a multiresolution analysis of $L^2(0,1)$, allowing fast wavelet transforms. We show in next section that in the context of compactly supported wavelets with polynomial reproduction, the spaces V_j^0, with associated scaling functions and wavelets can be simply constructed from the characteristics of the V_j^1-spaces. Furthermore our construction integrate homogeneous boundary conditions to the spaces V_j^1.
At this point, our construction differs radically from [19], where, inversely, the construction of V_j^1-spaces of $H_0^1(0,1)$ of derives from the integration of 1D MRAs of L^2-functions with zero mean, and finally need to complete the divergence-free basis with directionally constant functions.

The outline of the paper is as follows: in Section 2 we construct new V_j^0 spaces and wavelets by differentiating standard BMRAs of $H^1(0,1)$, as predicted by Jouini-Lemarié Rieusset theory. Section 3 introduces our finite dimensional divergence-free spaces and associated wavelets. Examples on wavelets and incompressible vector flow analysis show the feasibility of the method.

2. Construction of BMRAs on [0, 1] linked by differentiation

2.1. The fundamental construction of Jouini and Lemarié-Rieusset

The existence of divergence-free wavelet bases on the whole space $\mathbb{R}^d$ follows from the fundamental proposition of Lemarié-Rieusset [15]:

Proposition 1. *Let $(V_j^1(\mathbb{R}), \tilde{V}_j^1(\mathbb{R}))$ be a biorthogonal MRA of $L^2(\mathbb{R})$, with compactly supported scaling functions $(\varphi^1, \tilde{\varphi}^1)$ and wavelets $(\psi^1, \tilde{\psi}^1)$, such that $\varphi^1, \psi^1 \in C^{1+\varepsilon}$ for $\varepsilon > 0$. Then there exists a biorthogonal MRA $(V_j^0(\mathbb{R}), \tilde{V}_j^0(\mathbb{R}))$, with associated scaling functions $(\varphi^0, \tilde{\varphi}^0)$ and wavelets $(\psi^0, \tilde{\psi}^0)$, such that:*
$(\varphi^1)'(x) = \varphi^0(x) \ - \ \varphi^0(x-1)$ and $(\psi^1)' \ = \ 4 \ \psi^0$.
The dual functions verify: $\int_x^{x+1} \tilde{\varphi}^1(t) \, dt = \tilde{\varphi}^0(x)$ and $(\tilde{\psi}^0)' \ = \ -4 \ \tilde{\psi}^1$.

From the generators $(\varphi^1, \tilde{\varphi}^1)$, $(\varphi^0, \tilde{\varphi}^0)$ of Proposition 1, Jouini and Lemarié-Rieusset prove the existence of two one-dimensional MRA of $L^2(0,1)$, (V_j^1) and (V_j^0) linked by differentiation [11]:

$$\frac{d}{dx} V_j^1 \quad = \quad V_j^0. \tag{3}$$

Moreover the biorthogonal spaces should satisfy:

$$\tilde{V}_j^0 \quad = \quad H_0^1(0,1) \cap \int_0^x \tilde{V}_j^1 = \left\{ f \ : \ f' \in \tilde{V}_j^1 \text{ and } \ f(0) = f(1) = 0 \right\}. \tag{4}$$

Our objective in the rest of the section is to provide an effective construction of such multiresolution analyses, which enables vanishing boundary conditions, and fast wavelet algorithms for practical computations. We begin by recalling the basic setting of MRAs of $H^1(0,1)$ and $H_0^1(0,1)$, then we propose a practical computation of the spaces $(V_j^0, \tilde{V}_j^0)$.

2.2. Regular MRA $(V_j^1, \tilde{V}_j^1)$ of $L^2(0,1)$ with polynomial reproduction $(r, \tilde{r})$, and associated MRA $(V_j^D, \tilde{V}_j^D)$ of $H_0^1(0,1)$

The construction of spaces $(V_j^1, \tilde{V}_j^1)$ is classical and based on biorthogonal multiresolution analyses on the interval reproducing polynomials up to some degree $r-1$ in V_j^1 and $\tilde{r}-1$ in $\tilde{V}_j^1$ [5, 6, 10]: the principle is to start with generators $(\varphi^1, \tilde{\varphi}^1)$, that are biorthogonal scaling functions of a BMRA on $\mathbb{R}$. We suppose that φ^1 is $C^{1+\varepsilon}$, $\varepsilon > 0$, compactly supported on $[n_{min}, n_{max}]$ (n_{min}, n_{max} integers), and reproduces polynomials up to degree $r-1$:

$$0 \leq \ell \leq r-1, \quad \frac{x^\ell}{\ell!} = \sum_{k=-\infty}^{+\infty} \tilde{p}_\ell^1(k) \ \varphi^1(x-k), \quad \forall \ x \in \mathbb{R}, \tag{5}$$

with $\tilde{p}_\ell^1(k) = \langle \frac{x^\ell}{\ell!}, \tilde{\varphi}^1(x-k) \rangle$. Similarly, $\tilde{\varphi}^1$ reproduces polynomials up to degree $\tilde{r}-1$ and we note $p_\ell^1(k) = \langle \frac{x^\ell}{\ell!}, \varphi^1(x-k) \rangle$. For j sufficiently large, the spaces V_j^1 on $[0,1]$ have the structure:

$$V_j^1 = V_j^{1,\flat} \oplus V_j^{1,int} \oplus V_j^{1,\sharp}, \tag{6}$$

where $V_j^{1,int} = span\{\varphi_{j,k}^1(x) = 2^{j/2} \varphi^1(2^j x - k) \ ; \ k = k_\flat, \ 2^j - k_\sharp\}$ is the space generated by *interior scaling functions* whose supports are included into $[\frac{\delta_\flat}{2^j}, 1 -$

$\frac{\delta_\sharp}{2^j}] \subset [0,1]$ ($\delta_\flat,\ \delta_\sharp \in \mathbb{N}$ be two fixed parameters), and $k_\flat = \delta_\flat - n_{min}$ and $k_\sharp = \delta_\sharp + n_{max}$. Moreover

$$V_j^{1,\flat} = span\{\Phi_{j,\ell}^{1,\flat}(x) = 2^{j/2}\Phi_\ell^{1,\flat}(2^j x)\ ;\ \ell = 0, \cdots, r-1\},$$
$$V_j^{1,\sharp} = span\{\Phi_{j,\ell}^{1,\sharp}(1-x) = 2^{j/2}\Phi_\ell^{1,\sharp}(2^j(1-x))\ ;\ \ell = 0, \cdots, r-1\},$$

are the *edge spaces*, the *edge scaling functions* at the edge 0 being defined in order to preserve the polynomial reproduction (5) on the interval $[0,1]$:

$$0 \le \ell \le r-1, \quad \Phi_\ell^{1,\flat}(x) = \sum_{k=1-n_{max}}^{k_\flat - 1} \tilde{p}_\ell^1(k)\ \varphi^1(x-k)\ \chi_{[0,+\infty[}. \tag{7}$$

At the edge 1, the edge scaling functions $\Phi_{j,\ell}^{1,\sharp}$ are constructed on $]-\infty, 1]$ by symmetry, using the transform $Tf(x) = f(1-x)$. In practice we have to choose $j \ge j_{min}$ where j_{min} is the smallest integer which verifies $j_{min} > \log_2[n_{max} - n_{min} + \delta_\sharp + \delta_\flat]$ to ensure that the supports of edge scaling functions at 0 do not intersect the supports of edge scaling functions at 1.

The polynomial reproduction in V_j^1 is then satisfied since, for $0 \le \ell \le r-1$ and $x \in [0,1]$ we have:

$$\frac{2^{j/2}(2^j x)^\ell}{\ell!} = 2^{j/2}\Phi_\ell^{1,\flat}(2^j x) + \sum_{k=k_\flat}^{2^j - k_\sharp} \tilde{p}_\ell^1(k)\ \varphi_{j,k}^1(x) + 2^{j/2}\Phi_\ell^{1,\sharp}(2^j(1-x)). \tag{8}$$

Similarly, the biorthogonal spaces $\tilde{V}_j^1$ are defined with the same structure, allowing the polynomial reproduction up to degree $\tilde{r}-1$:

$$\tilde{V}_j^1 = span\{\tilde{\Phi}_{j,\ell}^{1,\flat}\}_{\ell=0,\tilde{r}-1} \oplus \tilde{V}_j^{1,int} \oplus span\{\tilde{\Phi}_{j,\ell}^{1,\sharp}\}_{\ell=0,\tilde{r}-1}, \tag{9}$$

where $\tilde{V}_j^{1,int} = span\{\tilde{\varphi}_{j,k}^1\ ;\ k = \tilde{k}_\flat,\ 2^j - \tilde{k}_\sharp\}$ is the space generated by interior scaling functions $\tilde{\varphi}_{j,k}^1(x) = 2^{j/2}\tilde{\varphi}^1(2^j x - k)$, whose supports are included into $[\frac{\tilde{\delta}_\flat}{2^j}, 1 - \frac{\tilde{\delta}_\sharp}{2^j}]$ ($\tilde{\delta}_\flat,\ \tilde{\delta}_\sharp \in \mathbb{N}$ be two parameters). The edge scaling functions at 0 are defined by:

$$0 \le \ell \le \tilde{r}-1, \quad \tilde{\Phi}_\ell^{1,\flat}(x) = \sum_{k=1-\tilde{n}_{max}}^{\tilde{k}_\flat - 1} p_\ell^1(k)\ \tilde{\varphi}^1(x-k)\ \chi_{[0,+\infty[}. \tag{10}$$

The equality between dimensions of V_j^1 and $\tilde{V}_j^1$ is obtained by adjusting the parameters $\tilde{k}_\flat = \tilde{\delta}_\flat - \tilde{n}_{min}$ and $\tilde{k}_\sharp = \tilde{\delta}_\sharp + \tilde{n}_{max}$ (with $[\tilde{n}_{min}, \tilde{n}_{max}] = supp\ \tilde{\varphi}^1$, $\tilde{n}_{min}$, $\tilde{n}_{max}$ integers) such that: $\Delta_j = \dim(V_j^1) = \dim(\tilde{V}_j^1) = 2^j - (\delta_\flat + \delta_\sharp) - (n_{max} - n_{min}) + 2r + 1$. Remark that ($\delta_\flat,\ \delta_\sharp$) remain "free" parameters of the construction (often chosen equal to 0 or 1). The last step of the construction lies in the biorthogonalization process of the basis functions, since edge scaling functions of V_j^1 and $\tilde{V}_j^1$ are no more biorthogonal [2, 6, 10, 17]. Finally, the spaces $(V_j^1, \tilde{V}_j^1)$ form a biorthogonal MRA of $L^2(0,1)$.

A MRA of $H_0^1(0,1)$ can be simply defined from (V_j^1) by $V_j^D = V_j^1 \cap H_0^1(0,1)$. As described in [4, 16, 17], it suffices to remove the edge scaling functions $\Phi_0^{1,\flat}$ defined in (7) at edge 0 and $\Phi_0^{1,\sharp}$ at edge 1 which leads to:

$$V_j^D = span\{\Phi_{j,\ell}^{1,\flat} \ ; \ \ell = 1, r-1\} \oplus V_j^{1,int} \oplus span\{\Phi_{j,\ell}^{1,\sharp} \ ; \ \ell = 1, r-1\}.$$

To simplify, we denote by $\varphi_{j,k}^D$ the scaling functions of V_j^D:

$$V_j^D = span\{\varphi_{j,k}^D \ ; \ k = 1, \ \Delta_j - 2\}.$$

In such case, we also remove the edge functions $\tilde{\Phi}_0^{1,\flat}$ and $\tilde{\Phi}_0^{1,\sharp}$ defined in (10) from $\tilde{V}_j^1$, to adjust the dimension of the biorthogonal space:

$$\tilde{V}_j^D = span\{\tilde{\Phi}_{j,\ell}^{1,\flat}\}_{\ell=1,\tilde{r}-1} \oplus \tilde{V}_j^{1,int} \oplus span\{\tilde{\Phi}_{j,\ell}^{1,\sharp}\}_{\ell=1,\tilde{r}-1} \tag{11}$$

After a biorthogonalization process, we finally note:

$$\tilde{V}_j^D = span\{\tilde{\varphi}_{j,k}^D \ ; \ k = 1, \ \Delta_j - 2\}$$

and the spaces $(V_j^D, \tilde{V}_j^D)$ form a biorthogonal MRA of $H_0^1(0,1)$.

2.3. Construction of $(V_j^0, \tilde{V}_j^0)$ linked by differentiation /integration with $(V_j^1, \tilde{V}_j^1)$

We now construct spaces $(V_j^0, \tilde{V}_j^0)$, that will be related to the spaces $(V_j^1, \tilde{V}_j^1)$ of Section 2.2 by relations (3,4) of differentiation/integration. In practice, we follows the same structure of construction, starting from generators $(\varphi^0, \tilde{\varphi}^0)$ arising from Proposition 1. Recalling that $\frac{d}{dx}\varphi^1(x) = \varphi^0(x) - \varphi^0(x-1)$, φ^0 has for compact support $[n_{min}, n_{max} - 1]$, and reproduces polynomials up to degree $r-2$:

$$0 \le \ell \le r-2, \quad \frac{x^\ell}{\ell!} = \sum_{k=-\infty}^{+\infty} \tilde{p}_\ell^0(k) \ \varphi^0(x-k), \tag{12}$$

with $\tilde{p}_\ell^0(k) = \langle \frac{x^\ell}{\ell!}, \tilde{\varphi}^0(x-k) \rangle = \tilde{p}_{\ell+1}^1(k) - \tilde{p}_{\ell+1}^1(k-1)$ for $\ell = 0, \cdots, r-2$.
From Proposition 1, the scaling function $\tilde{\varphi}^0(x) = \int_x^{x+1} \tilde{\varphi}^1(t)dt$ has for compact support $[\tilde{n}_{min} - 1, \tilde{n}_{max}]$, and reproduces polynomials up to degree $\tilde{r}$. Noting $p_\ell^0(k) = \langle \frac{x^\ell}{\ell!}, \varphi^0(x-k) \rangle$, we have $p_\ell^1(k) = p_{\ell+1}^0(k+1) - p_{\ell+1}^0(k)$ for $\ell = 1, \cdots, \tilde{r}$.

Like V_j^1, multiresolution spaces V_j^0 are defined to ensure the polynomial reproduction on $[0,1]$ up to degree $r-2$: $V_j^0 = V_j^{0,\flat} \oplus V_j^{0,int} \oplus V_j^{0,\sharp}$
where $V_j^{0,int} = span\{\varphi_{j,k}^0(x) = 2^{j/2}\varphi^0(2^j x - k) \ ; \ k = k_\flat, \ 2^j - k_\sharp + 1\}$ is generated by interior scaling functions whose supports are included into $[\frac{\delta_\flat}{2^j}, 1 - \frac{\delta_\sharp}{2^j}] \subset [0,1]$, the parameters $\delta_\flat$, $\delta_\sharp$ being chosen *equal* to those arising from the construction of V_j^1 . The edge spaces

$$V_j^{0,\flat} = span\{\Phi_{j,\ell}^{0,\flat}(x) = 2^{j/2}\Phi_\ell^{0,\flat}(2^j x) \ ; \ \ell = 0, \cdots, r-2\},$$
$$V_j^{0,\sharp} = span\{\Phi_{j,\ell}^{0,\sharp}(1-x) = 2^{j/2}\Phi_\ell^{0,\sharp}(2^j(1-x)) \ ; \ \ell = 0, \cdots, r-2\},$$

are generated by the left *edge scaling functions*:

$$0 \le \ell \le r-2, \quad \Phi_\ell^{0,\flat}(x) = \sum_{k=2-n_{max}}^{k_\flat - 1} \tilde{p}_\ell^0(k)\ \varphi^0(x-k)\ \chi_{[0,+\infty[}.$$

Biorthogonal spaces $\tilde{V}_j^0$ are defined with similar structure, allowing a polynomial reproduction up to degree $\tilde{r}$, but satisfying *vanishing boundary conditions* at 0 and 1, to preserve the commutation between the derivation and the multiscale projectors [11]. Then:

$$\tilde{V}_j^0 = span\{\tilde{\Phi}_{j,\ell}^{0,\flat}\}_{\ell=1,\tilde{r}} \oplus \tilde{V}_j^{0,int} \oplus span\{\tilde{\Phi}_{j,\ell}^{1,\sharp}\}_{\ell=1,\tilde{r}}, \tag{13}$$

with $\tilde{V}_j^{0,int} = span\{\tilde{\varphi}_{j,k}^0\ ;\ k = \tilde{k}_\flat{+}1,\ 2^j - \tilde{k}_\sharp\}$, and $\tilde{\Phi}_\ell^{0,\flat} = \sum_{k=1-\tilde{n}_{max}}^{\tilde{k}_\flat} p_\ell^0(k)\ \tilde{\varphi}_k^0\ \chi_{[0,+\infty[}$, for $l = 1, \ldots, \tilde{r}$, be the left edge scaling functions vanishing at 0, the right edge scaling functions $\tilde{\Phi}_{j,\ell}^{0,\sharp}$ being constructed by symmetry. In next proposition we will need to use the edge scaling function non vanishing at 0, $\tilde{\Phi}_0^{0,\flat} = \sum_{k=1-\tilde{n}_{max}}^{\tilde{k}_\flat} \tilde{\varphi}_k^0\ \chi_{[0,+\infty[}$. In practice now j should satisfy $j > j_{min}$ with:
$j_{min} > \max\{\log_2[n_{max} - n_{min} + \delta_\sharp + \delta_\flat + 1], \log_2[\tilde{n}_{max} - \tilde{n}_{min} + \tilde{\delta}_\sharp + \tilde{\delta}_\flat + 1]\}$,
and a simple calculation shows that $\dim(V_j^0) = \dim(\tilde{V}_j^0) = \Delta_j - 1$.
The following proposition proves that $\frac{d}{dx} V_j^1 = V_j^0$ and $\frac{d}{dx}\tilde{V}_j^0 \subset \tilde{V}_j^1$.

Proposition 2.
(i) The interior scaling functions of (V_j^1, V_j^0) *and* $(\tilde{V}_j^1, \tilde{V}_j^0)$ *satisfy:*

$$\frac{d}{dx}(\varphi_{j,k}^1) = 2^j[\varphi_{j,k}^0 - \varphi_{j,k+1}^0],\ \frac{d}{dx}(\tilde{\varphi}_{j,k}^0) = 2^j[\tilde{\varphi}_{j,k-1}^1 - \tilde{\varphi}_{j,k}^1],\ \textit{for}\ \ k_\flat \le k \le 2^j - k_\sharp,$$

and $\dim(V_j^{0,int}) = \dim(V_j^{1,int}) + 1,\ \dim(\tilde{V}_j^{0,int}) = \dim(\tilde{V}_j^{1,int}) - 1$.
(ii) The edge scaling functions of (V_j^1, V_j^0) *satisfy, for* $\ell = 1, \ldots, r-1$*:*

$$(\Phi_0^{1,\flat})' = -\varphi_{k_\flat}^0, \qquad (\Phi_\ell^{1,\flat})' = \Phi_{\ell-1}^{0,\flat} - \tilde{p}_\ell^1(k_\flat - 1)\ \varphi_{k_\flat}^0,$$
$$(\Phi_0^{1,\sharp})'(1-x) = \varphi_{2-k_\sharp}^0(x), \quad (\Phi_\ell^{1,\sharp})'(1-x) = -\Phi_{\ell-1}^{0,\sharp}(1-x) + \tilde{p}_\ell^1(2-k_\sharp)\ \varphi_{2-k_\sharp}^0(x),$$

whereas those of $(\tilde{V}_j^1, \tilde{V}_j^0)$ *are linked by: for* $\ell = 1, \ldots, \tilde{r}-1$,

$$(\tilde{\Phi}_\ell^{0,\flat})' = \tilde{\Phi}_{\ell-1}^{1,\flat} - p_\ell^0(\tilde{k}_\flat)\ \tilde{\varphi}_{\tilde{k}_\flat}^1\ , \qquad (\tilde{\Phi}_\ell^{0,\sharp}(1-x))' = -\tilde{\Phi}_{\ell-1}^{1,\sharp}(1-x) + p_\ell^0(2-\tilde{k}_\sharp)\ \tilde{\varphi}_{1-\tilde{k}_\sharp}^1.$$

Moreover, the function $\tilde{\Phi}_0^{0,\flat}$ *verifies :* $(\tilde{\Phi}_0^{0,\flat})' = -\tilde{\varphi}_{\tilde{k}_\flat}^1$.

Proof. (i) follows directly from Proposition 1. (ii) comes from the definitions of edge scaling functions: we focus on the first line of equalities, at edge 0. We note in the following $\varphi_k^i(x) = \varphi^i(x-k)$ $(i = 0, 1)$.
For $\ell = 0$, differentiating equation (7) in $]0, +\infty[$, one obtains ($\tilde{p}_0^1(k) = 1, \forall k$):

$$(\Phi_0^{1,\flat})' = \sum_{k=1-n_{max}}^{k_\flat - 1} (\varphi_k^0 - \varphi_{k+1}^0)\ \chi_{]0,+\infty[} = \varphi_{1-n_{max}}^0\ \chi_{]0,+\infty[} - \varphi_{k_\flat}^0 = -\varphi_{k_\flat}^0,$$

since $supp\ \varphi^0_{1-n_{max}} = [n_{min} - n_{max} + 1, 0]$.
In the same way, for $\ell = 1, r-1$:

$$\begin{aligned}(\Phi^{1,\flat}_\ell)' &= \sum_{k=1-n_{max}}^{k_\flat - 1} \tilde{p}^1_\ell(k)\ (\varphi^0_k - \varphi^0_{k+1})\ \chi_{]0,+\infty[} \\ &= \sum_{k=2-n_{max}}^{k_\flat - 1} [\tilde{p}^1_\ell(k) - \tilde{p}^1_\ell(k-1)]\ \varphi^0_k \chi_{]0,+\infty[} - p^1_\ell(k_\flat - 1)\ \varphi^0_{k_\flat}.\end{aligned}$$

From (12), since $\tilde{p}^0_{\ell-1}(k) = \tilde{p}^1_\ell(k) - \tilde{p}^1_\ell(k-1)$ we get:

$$(\Phi^{1,\flat}_\ell)' = \sum_{k=2-n_{max}}^{k_\flat - 1} \tilde{p}^0_{\ell-1}(k)\ \varphi^0_k \chi_{]0,+\infty[} - \tilde{p}^1_\ell(k_\flat - 1)\ \varphi^0_{k_\flat} = \Phi^{0,\flat}_{\ell-1} - \tilde{p}^1_\ell(k_\flat - 1)\ \varphi^0_{k_\flat}.$$

The proof for edge scaling functions at edge 1 and in the biorthogonal spaces $\tilde{V}^1_j$ and $\tilde{V}^0_j$ is obtained with similar arguments. □

For easy reading, the bases of $(V^1_j, \tilde{V}^1_j)$ and $(V^0_j, \tilde{V}^0_j)$, arising after the biorthogonalization will be now denoted by $(\varphi^1_{j,k}, \tilde{\varphi}^1_{j,k})_{k=1,\Delta_j}$ and $(\varphi^0_{j,k}, \tilde{\varphi}^0_{j,k})_{k=1,\Delta_j-1}$. The following proposition proves that our constructed BMRAs take place in the theoretical framework [11].

Proposition 3. *The biorthogonal spaces* $(V^1_j, \tilde{V}^1_j)$ *and* $(V^0_j, \tilde{V}^0_j)$ *verify relations (3, 4):* $\frac{d}{dx} V^1_j = V^0_j$ *and* $\tilde{V}^0_j = H^1_0 \cap \int_0^x \tilde{V}^1_j$.

Proof. The inclusion $\frac{d}{dx} V^1_j \subset V^0_j$ is straightforward according to Proposition 2. The equality of dimensions between spaces leads to the first equality. Moreover Proposition 2 implies: $\int_0^x \tilde{V}^1_j = \tilde{V}^0_j \oplus span\{2^{j/2}\tilde{\Phi}^{0,\flat}_0(2^j x) - \tilde{\Phi}^{0,\flat}_0(0)\}$. Since for $j \geq j_{min}$, $\tilde{V}^0_j \subset H^1_0(0,1)$ and $2^{j/2}\Phi^{0,\flat}_0(2^j) - \Phi^{0,\flat}_0(0) = -\Phi^{0,\flat}_0(0) \neq 0$ we obtain the second equality. □

This result induces the commutation between multiscale projectors and differentiation. Let $\mathcal{P}^1_j$ be the oblique projector on V^1_j parallel to $(\tilde{V}^1_j)^\perp$, $\tilde{\mathcal{P}}^1_j$ its adjoint, and $\mathcal{P}^0_j$, $\tilde{\mathcal{P}}^0_j$ the biorthogonal projectors associated with $(V^0_j, \tilde{V}^0_j)$, we have [11]:

Proposition 4.
(i) $\forall\ f \in H^1(0,1)$, $\frac{d}{dx} \circ \mathcal{P}^1_j f = \mathcal{P}^0_j \circ \frac{d}{dx} f$,
(ii) $\forall\ f \in H^1_0(0,1)$, $\frac{d}{dx} \circ \tilde{\mathcal{P}}^0_j f = \tilde{\mathcal{P}}^1_j \circ \frac{d}{dx} f$.

We now define the change of basis matrices between the spaces $(\frac{d}{dx} V^1_j, \frac{d}{dx} \tilde{V}^0_j)$ and $(V^0_j, \tilde{V}^1_j)$, useful in numerical computations.

Definition 1. Let $(L^1_j, L^0_j, \tilde{L}^0_j)$ be the change of basis matrices defined by:

$$\frac{d}{dx}\varphi^1_{j,k} = \sum_{n=1}^{\Delta_j - 1} (L^1_j)_{k,n}\ \varphi^0_{j,n}, \qquad \frac{d}{dx}\tilde{\varphi}^0_{j,k} = \sum_{n=1}^{\Delta_j} (\tilde{L}^0_j)_{k,n}\ \tilde{\varphi}^1_{j,n}, \tag{14}$$

$$\text{and} \qquad -\int_0^x \varphi^0_{j,k} = \sum_{m=1}^{\Delta_j} (L^0_j)_{k,m}\ \varphi^1_{j,m}. \tag{15}$$

As we will see in Proposition 7, the matrices L^0_j and L^1_j will occur in the computation of wavelet filters, and their explicit expression is given by the following proposition.

Proposition 5.
Let L^0 and L^1 be the renormalized matrices: $L^1_j = 2^j L^1$ and $L^0_j = 2^{-j} L^0$. Then, L^1 is a rectangular matrix of size $\Delta_j \times (\Delta_j - 1)$ whose non zero elements are:

$$L^1_{k,k-1} = 1, \quad L^1_{k,k} = -1, \quad r+1 \le k \le \Delta_j - r$$

and for $2 \le k \le r$:

$$L^1_{1,r} = -1,\ L^1_{k,k-1} = 1,\ L^1_{k,r} = -\tilde{p}^1_{k-1}(k_\flat - 1)$$
$$L^1_{\Delta_j,\Delta_j-r} = 1,\ L^1_{\Delta_j-k+1,\Delta_j-k+1} = -1,\ L^1_{\Delta_j-k+1,\Delta_j-r} = \tilde{p}^1_{k-1}(2^j - k_\sharp + 1)$$

Similarly, L^0 is a rectangular matrix of size $(\Delta_j - 1) \times \Delta_j$ whose no zero elements are:

$$L^0_{k,m} = -1, \quad L^0_{k,\Delta_j} = -1, \quad k+1 \le m \le \Delta_j - r \text{ and } r \le k \le \Delta_j - r$$

and for $2 \le k \le r$:

$$L^0_{r,1} = 1,\ L^0_{k-1,k} = -1,\ L^0_{k-1,1} = \tilde{p}^1_{k-1}(k_\flat - 1)$$
$$L^0_{\Delta_j-r,\Delta_j} = -1,\ L^0_{\Delta_j-k+1,\Delta_j-k+1} = 1,\ L^0_{\Delta_j-k+1,\Delta_j} = -\tilde{p}^1_{k-1}(2^j - k_\sharp + 1)$$

2.3.1. Wavelet spaces

We first recall the structure of wavelet spaces of the BMRA $(V^1_j, \tilde{V}^1_j)$, which is classical, although different kinds of wavelets may be designed [2, 4, 5, 6, 17, 10]. As for the scaling functions construction, in V^1_{j+1} one must distinguish *interior wavelets* $\psi^1_{j,k}$ and edge wavelets denoted by $\Psi^{1,\flat}_{j,\ell}$ at edge 0 and $\Psi^{1,\sharp}_{j,\ell}$ at edge 1. The interior wavelets $\psi^1_{j,k}$ correspond to wavelets on $\mathbb{R}$ whose supports are included into $[\frac{\delta_\flat}{2^{j+1}}, 1 - \frac{\delta_\sharp}{2^{j+1}}]$. Since the the support of ψ^1 (wavelet on $\mathbb{R}$) is $[\frac{n_{min} - \tilde{n}_{max} + 1}{2}, \frac{n_{max} - \tilde{n}_{min} + 1}{2}]$, a simple calculation [6, 10] shows that it suffices to take $k = p_\flat,\ 2^j - p_\sharp - 1$, where $p_\flat$ and $p_\sharp$ are integers defined by:

$$p_\flat = \lfloor \frac{\tilde{n}_{max} + k_\flat - 1}{2} \rfloor \qquad \text{and} \qquad p_\sharp = \lfloor \frac{k_\sharp - \tilde{n}_{min} + 1}{2} \rfloor.$$

For the edge wavelets it is important to have good localization. An example, proposed by [10] and used in our numerical tests, is to construct edge-wavelets of smallest support, which gives :

$$\Psi^{1,\flat}_{j,\ell} := \left(I - \mathcal{P}^1_j - \mathcal{Q}^{1,int}_j \right) \varphi^1_{j+1,k_\flat+2\ell}, \qquad \ell = 0, \ldots, p_\flat - 1, \tag{16}$$

and

$$\Psi^{1,\sharp}_{j,\ell} := \left(I - \mathcal{P}^1_j - \mathcal{Q}^{1,int}_j\right)\varphi^1_{j+1,2^{j+1}-k_\sharp-2\ell}, \qquad \ell = 0,\dots,p_\sharp - 1, \tag{17}$$

with $\mathcal{Q}^{1,int}_j$ the biorthogonal projector onto interior wavelets:

$$\mathcal{Q}^{1,int}_j(f) := \sum_{p_\flat \le k \le 2^j - p_\sharp - 1} \langle f, \tilde{\psi}^1_{j,k}\rangle \psi^1_{j,k}$$

Then, the biorthogonal wavelet spaces associated to V^1_j are defined by $W^1_j = V^1_{j+1} \cap (\tilde{V}^1_j)^\perp$ and, for $j \ge j_{min}$, have the form: $W^1_j = W^{1,\flat}_j \oplus W^{1,int}_j \oplus W^{1,\sharp}_j$,

$$\text{with} \begin{cases} W^{1,\flat}_j &= span\{\Psi^{1,\flat}_{j,\ell}(x) = 2^{j/2}\Psi^{1,\flat}_\ell(2^j x)\ ;\ \ell = 0,\ p_\flat - 1\}, \\ W^{1,int}_j &= span\{\psi^1_{j,k} = 2^{j/2}\psi^1(2^j x - k)\ ;\ k = p_\flat,\ 2^j - p_\sharp - 1\}, \\ W^{1,\sharp}_j &= span\{\Psi^{1,\sharp}_{j,\ell}(1-x) = 2^{j/2}\Psi^{1,\sharp}_\ell(2^j(1-x))\ ;\ \ell = 0,\ p_\sharp - 1\}, \end{cases}$$

The biorthogonal spaces $\tilde{W}^1_j$ are constructed in the same way, finally the wavelet bases of the two spaces must to be biorthogonalized identically as the scaling functions. The resulting wavelet bases are denoted by $\{\psi^1_{j,k}\}_{k=1,2^j}$ and $\{\tilde{\psi}^1_{j,k}\}_{k=1,2^j}$ without distinction.
The objective now is to exhibit biorthogonal wavelets of W^0_j and $\tilde{W}^0_j$, linked to $\psi^1_{j,k}$ and $\tilde{\psi}^1_{j,k}$ by differentiation/integration. This is done by the following proposition, established in the general framework by [11]:

Proposition 6. *Let $(V^1_j, \tilde{V}^1_j)$ and $(V^0_j, \tilde{V}^0_j)$ BMRAs satisfying proposition 3. The wavelet spaces $W^0_j = V^0_{j+1} \cap (\tilde{V}^0_j)^\perp$ and $\tilde{W}^0_j = \tilde{V}^0_{j+1} \cap (V^0_j)^\perp$ are linked to the biorthogonal wavelet spaces associated to $(V^1_j, \tilde{V}^1_j)$ by:*

$$W^0_j = \frac{d}{dx} W^1_j \quad \text{and} \quad \tilde{W}^0_j = \int_0^x \tilde{W}^1_j. \tag{18}$$

Moreover, let $\{\psi^1_{j,k}\}_{k=1,2^j}$ and $\{\tilde{\psi}^1_{j,k}\}_{k=1,2^j}$ be two biorthogonal wavelet bases of W^1_j and $\tilde{W}^1_j$. Biorthogonal wavelet bases of W^0_j and $\tilde{W}^0_j$ are directly defined by:

$$\psi^0_{j,k} = 2^{-j}(\psi^1_{j,k})' \quad \text{and} \quad \tilde{\psi}^0_{j,k} = -2^j \int_0^x \tilde{\psi}^1_{j,k}. \tag{19}$$

Interior wavelets $\psi^0_{j,k}(x) = 2^{j/2}\psi^0(2^j x - k)$ in this definition correspond to classical wavelets, ψ^0 being a wavelet on $\mathbb{R}$ associated to the scaling function φ^0 as in Proposition 1. On the other hand, in standard constructions [4, 5, 6, 17, 10], the edge wavelets of $W^0_j, \tilde{W}^0_j$ do not verify the relations (19). The next proposition guarantees that this new edge wavelets preserve fast algorithms since they satisfy two-scale equations.

Proposition 7. *Let $\{\psi^1_{j,k}\}_{k=1,2^j}$ and $\{\tilde{\psi}^1_{j,k}\}_{k=1,2^j}$ be two biorthogonal wavelet bases of W^1_j and $\tilde{W}^1_j$ associated respectively to filters G^1_j and $\tilde{G}^1_j$:*

$$\psi^1_{j,k} = \sum_n (G^1_j)_{k,n}\ \varphi^1_{j+1,n} \quad \textit{and} \quad \tilde{\psi}^1_{j,k} = \sum_n (\tilde{G}^1_j)_{k,n}\ \tilde{\varphi}^1_{j+1,n}.$$

Then there exist sparse matrices G^0_j and $\tilde{G}^0_j$ defined by:

$$G^0_j = 2^{-j} G^1_j L^1_{j+1} \quad \textit{and} \quad \tilde{G}^0_j = -2^j \tilde{G}^1_j L^{0T}_{j+1}, \tag{20}$$

such that the wavelets $\psi^0_{j,k}$ and $\tilde{\psi}^0_{j,k}$ satisfy:

$$\psi^0_{j,k} = \sum_n (G^0_j)_{k,n} \varphi^0_{j+1,n} \quad \textit{and} \quad \tilde{\psi}^0_{j,k} = \sum_n (\tilde{G}^0_j)_{k,n} \tilde{\varphi}^0_{j+1,n}.$$

Remark 1. The above construction of wavelets $\psi^0_{j,k}$ and $\tilde{\psi}^0_{j,k}$ has two main interests: their filters are directly accessible from those of $\psi^1_{j,k}$ and $\tilde{\psi}^1_{j,k}$, and there is no need for biorthogonalization as for classical constructions. A MATLAB code computing corresponding low and high pass filters for several class of wavelet families can be downloaded from [14].

Proof. From the definition of wavelets (19) and of the change of basis (definition 1):

$$2^j \psi^0_{j,k} = \sum_n (G^1_j)_{k,n} (\varphi^1_{j+1,n})' = \sum_{n,m} (G^1_j)_{k,n} (L^1_{j+1})_{n,m} \varphi^0_{j+1,m} = \sum_m [G^1_j L^1_{j+1}]_{k,m} \varphi^0_{j+1,m},$$

since $\psi^0_{j,k} = \sum_m (G^0_j)_{k,m} \varphi^0_{j+1,m}$, we obtain G^0_j. $\tilde{G}^0_j$ is obtained similarly. □

Example 1. Figure 1 shows the plots of edge scaling functions and wavelets at 0 in V^1_j (left), and V^0_j (right). The generators $(\varphi^1, \tilde{\varphi}^1)$ used are biorthogonal B-Splines with $r = \tilde{r} = 3$, $n_{min} = -1$, $n_{max} = 2$, $\tilde{n}_{min} = -3$ and $\tilde{n}_{max} = 4$. The "free" integer parameters are chosen as $\delta_\flat = \delta_\sharp = 2$ and $\tilde{\delta}_\flat = \tilde{\delta}_\sharp = 0$.

3. Divergence-free scaling functions and wavelets on the square

3.1. Construction of divergence-free MRA of $\mathcal{H}_{div}(\Omega)$

Let $\Omega = [0,1]^2$. The aim of the present section is to provide a divergence-free MRA and wavelet bases of the space $\mathcal{H}_{div}(\Omega)$, introduced in (1). Since $\mathcal{H}_{div}(\Omega)$ is also equal to (2), our construction consists in taking the curl of a regular MRA of the space $H^1_0(\Omega)$. Such MRA is given by the tensor-product $V^D_j \otimes V^D_j$ of a regular MRA of $H^1_0(0,1)$:$V^D_j = V^1_j \cap H^1_0(0,1)$, as constructed in Section 2. With the notations $V^D_j = span\{\varphi^D_{j,k}\ ;\ k = 1, \Delta_j - 2\}$, and $\psi^D_{j,k}$ the corresponding wavelets, we define the divergence-free scaling function spaces.

Definition 2. For $j \geq j_{min}$, the *divergence-free scaling function spaces* $\mathbf{V}_j^{div}$ are defined by:

$$\mathbf{V}_j^{div} = \mathbf{curl}(V_j^D \otimes V_j^D) = span\{\Phi_{j,\mathbf{k}}^{div}\}, \tag{21}$$

where the *divergence-free scaling functions* are given by[1]:

$$\Phi_{j,\mathbf{k}}^{div} := \frac{1}{\sqrt{2}}\mathbf{curl}[\varphi_{j,k_1}^D \otimes \varphi_{j,k_2}^D] = \frac{1}{\sqrt{2}}\left(\varphi_{j,k_1}^D \otimes (\varphi_{j,k_2}^D)', -(\varphi_{j,k_1}^D)' \otimes \varphi_{j,k_2}^D\right). \tag{22}$$

The spaces $\mathbf{V}_j^{div}$ defined above constitute an increasing sequence in $(L^2(\Omega))^2$: $\mathbf{V}_j^{div} \subset \mathbf{V}_{j+1}^{div}$, of dimension: $\dim(\mathbf{V}_j^{div}) = \dim(V_j^D)^2 = (\Delta_j - 2)^2$. We will also consider the more standard MRA $\mathbf{V}_j$ of $(L^2(\Omega))^2$:

$$\mathbf{V}_j = (V_j^1 \otimes V_j^0) \times (V_j^0 \otimes V_j^1), \tag{23}$$

V_j^0 being the spaces defined in Section 2.3. By Proposition 3, these discrete spaces $\mathbf{V}_j$ preserve the divergence-free condition, as stated in [11]:

$$\mathbf{u} \in (L^2(\Omega))^2, \;\; \mathbf{div}(\mathbf{u}) = 0 \;\Rightarrow\; \mathbf{div}[\mathbf{P}_j(\mathbf{u})] = 0, \tag{24}$$

where $\mathbf{P}_j = (\mathcal{P}_j^1 \otimes \mathcal{P}_j^0, \mathcal{P}_j^0 \otimes \mathcal{P}_j^1)$ is the biorthogonal projector on $\mathbf{V}_j$. In the same way, we introduce anisotropic divergence-free wavelets and wavelet spaces:

Definition 3. For $j_1, j_2 \geq j_{min}$, the *anisotropic divergence-free wavelets and wavelet spaces* are defined by:

$$\Psi_{\mathbf{j},\mathbf{k}}^{div,1} := \frac{1}{\sqrt{4^{j_2}+1}}\mathbf{curl}[\varphi_{j_{min},k_1}^D \otimes \psi_{j_2,k_2}^D] \quad \text{and} \quad \mathbf{W}_{\mathbf{j}}^{div,1} = span\{\Psi_{\mathbf{j},\mathbf{k}}^{div,1}\},$$

$$\Psi_{\mathbf{j},\mathbf{k}}^{div,2} := \frac{1}{\sqrt{4^{j_1}+1}}\mathbf{curl}[\psi_{j_1,k_1}^D \otimes \varphi_{j_{min},k_2}^D] \quad \text{and} \quad \mathbf{W}_{\mathbf{j}}^{div,2} = span\{\Psi_{\mathbf{j},\mathbf{k}}^{div,2}\},$$

$$\Psi_{\mathbf{j},\mathbf{k}}^{div,3} := \frac{1}{\sqrt{4^{j_1}+4^{j_2}}}\mathbf{curl}[\psi_{j_1,k_1}^D \otimes \psi_{j_2,k_2}^D] \quad \text{and} \quad \mathbf{W}_{\mathbf{j}}^{div,3} = span\{\Psi_{\mathbf{j},\mathbf{k}}^{div,3}\}.$$

We now prove the main result of the article, that is $(\mathbf{V}_j^{div})_{j \geq j_{min}}$ is a multiresolution analysis of $\mathcal{H}_{div}(\Omega)$.

Proposition 8. *The divergence-free scaling function spaces* $\mathbf{V}_j^{div}$ *and wavelet spaces* $\mathbf{W}_{\mathbf{j}}^{div,\varepsilon}$ *for* $\varepsilon = 1, 2, 3$*, satisfy:*
(i) $\mathbf{V}_{j_{min}}^{div} \subset \cdots \subset \mathbf{V}_j^{div} \subset \mathbf{V}_{j+1}^{div} \subset \cdots \subset \mathcal{H}_{div}(\Omega)$ *and* $\overline{\cup \mathbf{V}_j^{div}} = \mathcal{H}_{div}(\Omega)$.
(ii) $\mathbf{V}_j^{div} = \mathbf{V}_{j_{min}}^{div} \bigoplus_{j_{min} \leq j_1, j_2 \leq j-1} (\oplus_{\varepsilon=1,2,3} \mathbf{W}_{\mathbf{j}}^{div,\varepsilon})$.
(iii) The set $\{\Phi_{j_{min},\mathbf{k}}^{div}, \Psi_{\mathbf{j},\mathbf{k}}^{div,\varepsilon}\}_{j_1,j_2 \geq j_{min},\ \varepsilon=1,2,3}$ *is a Riesz basis of* $\mathcal{H}_{div}(\Omega)$.

[1] The **curl** of a 2D scalar function Ψ is defined by $\mathbf{curl}\ \Psi = (\frac{\partial \Psi}{\partial y}, -\frac{\partial \Psi}{\partial x})$.

Then each vector function $\mathbf{u}$ of $\mathcal{H}_{div}(\Omega)$ has a unique decomposition:

$$\mathbf{u} = \sum_{\mathbf{k}} c^{div}_{j_{min},\mathbf{k}} \Phi^{div}_{j_{min},\mathbf{k}} + \sum_{\mathbf{j},\mathbf{k}} \sum_{\varepsilon=1,2,3} d^{div,\varepsilon}_{\mathbf{j},\mathbf{k}} \Psi^{div,\varepsilon}_{\mathbf{j},\mathbf{k}}, \tag{25}$$

with the norm-equivalence: $\|\mathbf{u}\|^2_{L^2} \sim \sum_{\mathbf{k}} |c^{div}_{j_{min},\mathbf{k}}|^2 + \sum_{\mathbf{j},\mathbf{k}} \sum_{\varepsilon=1,2,3} |d^{div,\varepsilon}_{\mathbf{j},\mathbf{k}}|^2$.

Proof. (i) Let $\mathbf{V}_j$ be the spaces defined in (23). Since the spaces $\mathcal{H}_{div}(\Omega) \cap \mathbf{V}_j$ provide a multiresolution analysis of $\mathcal{H}_{div}(\Omega)$ [11], (i) is reduced to prove $\mathbf{V}^{div}_j = \mathcal{H}_{div}(\Omega) \cap \mathbf{V}_j$.
According to Proposition 2, we have $\mathbf{V}^{div}_j \subset \mathbf{V}_j$ and $\mathbf{V}^{div}_j \subset \mathcal{H}_{div}(\Omega)$ by construction. Conversely, let $\mathbf{u} \in \mathcal{H}_{div}(\Omega) \cap \mathbf{V}_j$, and $\mathbf{P}_j$ the biorthogonal projector on $\mathbf{V}_j$. We are going to prove that $\mathbf{u} \in \mathbf{V}^{div}_j$. On one hand, as $\mathbf{u} \in \mathbf{V}_j$ we have $\mathbf{u} = \mathbf{P}_j(\mathbf{u})$, on the other hand due to $\mathbf{u} \in \mathcal{H}_{div}(\Omega)$ we have $\mathbf{u} = \mathbf{curl}\ (\chi)$ with $\chi \in H^1_0(\Omega)$, and thus $\mathbf{u} = \mathbf{P}_j[\mathbf{curl}\ (\chi)]$. Since the spaces $(V^D_j \otimes V^D_j)_{j \geq j_{min}}$ form a MRA of $H^1_0(\Omega)$, we can decompose χ as:

$$\chi = P^D_j(\chi) + \sum_{j_1,j_2 \geq j} \left(Q^D_{1,\mathbf{J}}(\chi) + Q^D_{2,\mathbf{J}}(\chi) + Q^D_{3,\mathbf{J}}(\chi) \right), \quad (\mathbf{J} = (j_1, j_2))$$

$$\text{where} \quad P^D_j(\chi) = \sum_{\mathbf{k}} c_{\mathbf{k}}\ \varphi^D_{j,k_1} \otimes \varphi^D_{j,k_2}, \qquad Q^D_{2,\mathbf{J}}(\chi) = \sum_{j_1 \geq j} \sum_{\mathbf{k}} d^2_{j_1,\mathbf{k}}\ \psi^D_{j_1,k_1} \otimes \varphi^D_{j,k_2},$$

$$Q^D_{1,\mathbf{J}}(\chi) = \sum_{j_2 \geq j} \sum_{\mathbf{k}} d^1_{j_2,\mathbf{k}}\ \varphi^D_{j,k_1} \otimes \psi^D_{j_2,k_2}, \qquad Q^D_{3,\mathbf{J}}(\chi) = \sum_{j_1,j_2 \geq j} \sum_{\mathbf{k}} d^3_{\mathbf{j},\mathbf{k}}\ \psi^D_{j_1,k_1} \otimes \psi^D_{j_2,k_2},$$

are the biorthogonal projectors on respectively $V^D_j \otimes V^D_j$, $W^D_{j_1} \otimes V^D_j$, $V^D_j \otimes W^D_{j_2}$ and $W^D_{j_1} \otimes W^D_{j_2}$. Proposition 2 implies that:

$$\mathbf{curl}\ [\varphi^D_{j,k_1} \otimes \psi^D_{j_2,k_2}] \in (V^D_j \otimes W^0_{j_2}) \times (V^0_j \otimes W^D_{j_2}),$$

hence: $\mathbf{P}_j(\mathbf{curl}\ [\varphi^D_{j,k_1} \otimes \psi^D_{j_2,k_2}]) = 0$, and same for $\mathbf{P}_j(\mathbf{curl}\ [\psi^D_{j_1,k_1} \otimes \varphi^D_{j,k_2}])$, $\mathbf{P}_j(\mathbf{curl}\ [\psi^D_{j_1,k_1} \otimes \psi^D_{j_2,k_2}])$. This leads to:

$$\mathbf{P}_j(\mathbf{curl}\ (\chi)) = \mathbf{P}_j(\mathbf{curl}\ [P^D_j(\chi)]) = \mathbf{curl}\ [P^D_j(\chi)].$$

By construction we have $\mathbf{curl}\ [P^D_j(\chi)] \in \mathbf{V}^{div}_j$, which implies $\mathbf{u} \in \mathbf{V}^{div}_j$ and then completes the proof: $\mathbf{V}^{div}_j = \mathcal{H}_{div}(\Omega) \cap \mathbf{V}_j$.
(ii) The spaces V^D_j form a MRA of $H^1_0(0,1)$, and we can write:

$$V^D_j \otimes V^D_j = (V^D_{j_{min}} \bigoplus_{j_1=j_{min}}^{j-1} W^D_{j_1}) \otimes (V^D_{j_{min}} \bigoplus_{j_2=j_{min}}^{j-1} W^D_{j_2}).$$

By definition of $\mathbf{V}^{div}_j$, we obtain:

$$\mathbf{V}^{div}_j = \mathbf{curl} \left[(V^D_{j_{min}} \otimes V^D_{j_{min}}) \bigoplus_{j_{min} \leq j_1,j_2 \leq j-1} [(V^D_{j_{min}} \otimes W^D_{j_2}) \oplus (W^D_{j_1} \otimes V^D_{j_{min}}) \oplus (W^D_{j_1} \otimes W^D_{j_2})] \right],$$

which leads to $\mathbf{V}_j^{div} = \mathbf{V}_{j_{min}}^{div} \bigoplus \left[\bigoplus_{j_{min} \le j_1, j_2 \le j-1} \left(\oplus_{\varepsilon=1,2,3} \mathbf{W}_{\mathbf{j}}^{div,\varepsilon} \right) \right]$.

(*iii*) First the completeness of the family $\{\Phi_{j_{min},\mathbf{k}}^{div}, \Psi_{\mathbf{j},\mathbf{k}}^{div,\varepsilon}\}_{j_1,j_2 \ge j_{min},\ \varepsilon=1,2,3}$ is ensured by points (i) and (ii). To prove the L^2-stability of the basis, we use a *vaguelette* argument, which is common in the wavelet theory, and recalled for instance in [11]. By assumption on 1D-spaces, the divergence-free wavelets $\Psi_{\mathbf{j},\mathbf{k}}^{div,\varepsilon}$ are compactly supported, zero mean value and belong to the space C^ϵ, for $\varepsilon > 0$: they constitute a vaguelette-familly, and the stability (leading to the norm-equivalence (25)) follows from the existence of a biorthogonal vavelet family for the $\Psi_{\mathbf{j},\mathbf{k}}^{div,\varepsilon}$, given by Proposition 9 below. □

We now construct a set biorthogonal divergence-free scaling functions and wavelets. Let:

$$\tilde{\Phi}_{j_{min},\mathbf{k}}^{div} := \frac{1}{\sqrt{2}} \begin{vmatrix} \tilde{\varphi}_{j_{min},k_1}^D \otimes \tilde{\gamma}_{j_{min},k_2} \\ -\tilde{\gamma}_{j_{min},k_1} \otimes \tilde{\varphi}_{j_{min},k_2}^D \end{vmatrix} \quad , \quad \tilde{\Psi}_{\mathbf{j},\mathbf{k}}^{div,1} := \frac{1}{\sqrt{4^{j_2}+1}} \begin{vmatrix} 2^{j_2} \tilde{\varphi}_{j_{min},k_1}^D \otimes \bar{\psi}_{j_2,k_2}^0 \\ -\tilde{\gamma}_{j_{min},k_1} \otimes \tilde{\psi}_{j_2,k_2}^D \end{vmatrix}$$

$$\tilde{\Psi}_{\mathbf{j},\mathbf{k}}^{div,2} := \frac{1}{\sqrt{4^{j_1}+1}} \begin{vmatrix} \tilde{\psi}_{j_1,k_1}^D \otimes \tilde{\gamma}_{j_{min},k_2} \\ -2^{j_1} \bar{\psi}_{j_1,k_1}^0 \otimes \tilde{\varphi}_{j_{min},k_2}^D \end{vmatrix} \quad , \quad \tilde{\Psi}_{\mathbf{j},\mathbf{k}}^{div,3} := \frac{1}{\sqrt{4^{j_1}+4^{j_2}}} \begin{vmatrix} 2^{j_2} \tilde{\psi}_{j_1,k_1}^D \otimes \bar{\psi}_{j_2,k_2}^0 \\ -2^{j_1} \bar{\psi}_{j_1,k_1}^0 \otimes \tilde{\psi}_{j_2,k_2}^D \end{vmatrix}$$

where $\tilde{\gamma}_{j_{min},k} = -\int_0^x \tilde{\varphi}_{j_{min},k}^D$ and $\bar{\psi}_{j,k}^0 = -2^{-j} \int_0^x \tilde{\psi}_{j,k}^D$, these wavelets corresponding to $\tilde{\psi}_{j,k}^0$ of (19) excepted for the edge functions. The following proposition is straightforward.

Proposition 9. *The families* $\left\{ \Phi_{j,\mathbf{k}}^{div}, \Psi_{\mathbf{j},\mathbf{k}}^{div,1}, \Psi_{\mathbf{j},\mathbf{k}}^{div,2}, \Psi_{\mathbf{j},\mathbf{k}}^{div,3} \ ;\ j_1, j_2 \ge j,\ \mathbf{k} \right\}$ *and* $\left\{ \tilde{\Phi}_{j,\mathbf{k}}^{div}, \tilde{\Psi}_{\mathbf{j},\mathbf{k}}^{div,1}, \tilde{\Psi}_{\mathbf{j},\mathbf{k}}^{div,2}, \tilde{\Psi}_{\mathbf{j},\mathbf{k}}^{div,3} \ ;\ j_1, j_2 \ge j,\ \mathbf{k} \right\}$ *are biorthogonal in* $(L^2(\Omega))^2$.

Example 2. Figure 2 shows the vector representation of divergence-free edge scaling functions **curl** $[\Phi_1^{1,\flat} \otimes \Phi_1^{1,\flat}]$, **curl** $[\Phi_2^{1,\flat} \otimes \Phi_2^{1,\flat}]$ and wavelets **curl** $[\Psi_1^{1,\flat} \otimes \Psi_1^{1,\flat}]$, **curl** $[\Psi_2^{1,\flat} \otimes \Psi_2^{1,\flat}]$, constructed from biorthogonal B-Spline generators $(\varphi^1, \tilde{\varphi}^1)$ with $r = \tilde{r} = 3$ used in example 1.

3.2. Incompressible vector flow analysis

As example, we consider a velocity field $\mathbf{u}$ of resolution 512^2, arising from a numerical simulation of lid driven cavity flow, computed in the approximation space $\mathbf{V}_9^{div}$ (see [12]). We computed its divergence-free decomposition (25), on divergence-free functions constructed with the B-Spline generators of Figure 1. Figure 3 shows the vector field $\mathbf{u}$ (left) and corresponding divergence-free coefficients. As expected, significant wavelet coefficients (left) are localized near shear zones.

In a second experiment, we computed the nonlinear approximation error provided by divergence-free wavelets, and compared it with this provided by standard wavelet decomposition of the velocity $\mathbf{u}$, and also with this provided by standard wavelet decomposition of the vorticity $\omega = curl\mathbf{u}$ (the vorticity is often preferred in numerical schemes to the velocity, since in 2D it is a scalar quantity; however the difficulty here is to impose boundary conditions on the

vorticity, whereas it is straightforward on the velocity [9]). Figure 4 (left) shows the relative L^2-error between $\mathbf{u}$ (or ω) and its N-best terms approximation, in function of N (in %): in $\mathbf{V}_9^{div}$ for $\mathbf{u}$, in $(V_9^D \otimes V_9^0) \times (V_9^0 \otimes V_1^0)$ for $\mathbf{u} = (u_1, u_2)$ and in $(V_9^1 \otimes V_9^1)$ for ω. Clearly the nonlinear error provided by the divergence-free wavelets behaves as well (or better) as the classical wavelet approximation for u and ω. But its main advantage lies in the preservation of the divergence-free property through the approximation step, which was also the case in the ω-formulation (but with the disadvantage of boundary conditions for ω): this is illustrated in Figure 4 (right), which plots the divergence of the N-best term approximation of u, with divergence-free wavelets, and with standard wavelets (the divergence has been computed with a Finite Difference scheme at grid points, which explains why it does not converge to exactly 0).

4. Conclusion

We have presented an effective construction of divergence-free MRAs and wavelets on the square. Our construction, based on MRA on the interval allowing polynomial reproduction, respects the theoretical framework established by Jouini and Lemarié-Rieusset [11]. Moreover it incorporates homogeneous boundary conditions in the basis functions, which allows the representation of the divergence-free space, with a free-slip boundary condition, and constitutes an alternative to the basis constructed by Stevenson [18]. Associated fast wavelet transforms can been implemented easily, since the basis functions verify simple two-scale equations. First realizations have been successfully presented in this article, and in [13] with the Helmholtz decomposition of a vector flow. Since $\mathcal{H}_{div}(\Omega)$ is already a curl-space in the cube $[0,1]^3$ [1], our construction extends readily to the 3D-case. Work on more complex problems are underway, such as the direct simulation of turbulence, this will be the subject of forthcoming papers.

Acknowledgements

V. Perrier acknowledges the support of the French Agence Nationale de la Recherche (ANR) under reference ANR-11-BS01-014-01 (TOMMI).

References

[1] Amrouche, C., Bernardi, C., Dauge, M., Girault, V.: Vector potentials in three dimensional nonsmooth domains. *Math. Meth. in the Applied Sciences* 21, 823–864 (1998)

[2] L. Andersson, N. Hall, B. Jawerth, G. Peters, Wavelets on closed subsets of the real line, *Recents Advances in Wavelets Analysis (L.L. Schumaker and G. Webb eds)*, Academic Press (1993) 1–61.

[3] G. Battle, P. Federbush, Divergence-free vector wavelets, *Michigan Math. Journ.* **40** (1993) 181–195.

[4] G. Chiavassa, J. Liandrat, On the Effective Construction of Compactly Supported Wavelets Satisfying Homogeneous Boundary Conditions on the Interval, *Appl. Comput. Harmon. Anal.* **4** (1997) 62–73.

[5] A. Cohen, I. Daubechies, P. Vial, Wavelets on the Interval and Fast Wavelet Transforms, *Appl. Comput. Harmon. Anal.* **1** (1993) 54–81.

[6] W. Dahmen, A. Kunoth, K. Urban, Biorthogonal Spline-wavelets on the interval. Stability and moment conditions, *App. Comput. Harmon. Anal.* **6** (1999) 132–196.

[7] E. Deriaz, V. Perrier, Divergence-free and curl-free wavelets in 2D and 3D, application to turbulent flows, *J. of Turbulence* **7(3)** (2006) 1–37.

[8] E. Deriaz, V. Perrier, Direct Numerical Simulation of Turbulence using divergence-free wavelets, *Multiscale Modeling & Simulation, SIAM* **7(3)** (2008) 1101–1129.

[9] V. Girault, P. A Raviart, *Finite element methods for Navier-Stokes equations*, Springer, Verlag Berlin (1986)

[10] S. Grivet-Talocia, A. Tabacco, Wavelets on the interval with optimal localization, *Math. Models. Meth. Appl. Sci.* **10(3)** (2000) 441–462.

[11] A. Jouini, P.G. Lemarié-Rieusset, Analyses multi-résolutions biorthogonales sur l'intervalle et applications, *Annales de l'I.H.P. Section C* **10** (1993) 453–476.

[12] S. Kadri-Harouna, *Ondelettes pour la prise en compte de conditions aux limites en turbulence incompressible*, Phd Thesis, Grenoble University, 2010.

[13] S. Kadri-Harouna, V. Perrier, Helmholtz-Hodge Decomposition on $[0,1]^d$ by Divergence-free and Curl-free Wavelets, J.-D Boissonat et (Eds), Curves and Surfaces, 2011, LNCS 6920, Springer Verlag Berlin Heidelberg (2011) 311–329.

[14] S. Kadri-Harouna, http://perso.univ-lr.fr/skadriha/Homepage/1D_functions.tar.gz.

[15] P.G. Lemarié-Rieusset, Analyses multi-résolutions non orthogonales, commutation entre projecteurs et dérivation et ondelettes vecteurs à divergence nulle, *Revista Matemática Iberoamericana* **8(2)** (1992) 221–236.

[16] R. Masson, Biorthogonal spline wavelets on the interval for the resolution of boundary problems. *M3AS* **6** (6) 749–791, 1996.

[17] P. Monasse, V. Perrier, Orthogonal Wavelet Bases Adapted For Partial Differential Equations With Boundary Conditions, *SIAM J.Math. Anal.* **29** (1998) 1040–1065.

[18] R. Stevenson, Divergence-free wavelet bases on the hypercube, *Appl. Comput. Harmon. Anal.* (2010), **30**, 1–19.

[19] R. Stevenson, Divergence-free wavelet bases on the hypercube: Free-slip boundary conditions, and applications for solving the instationary Stokes equations. *Math. Comp.* 80, 1499–1523 (2011).

[20] K. Urban, *On divergence-free wavelets*, Advances in Computational Mathematics, **4**: 51-81, 1995.

[21] K. Urban, Wavelet Bases in H(div) and H($curl$), *Math. Comput.* **70** (2000) 739–766.

[22] K. Urban, *Wavelets in Numerical Simulation*, (Springer Berlin, 2002).

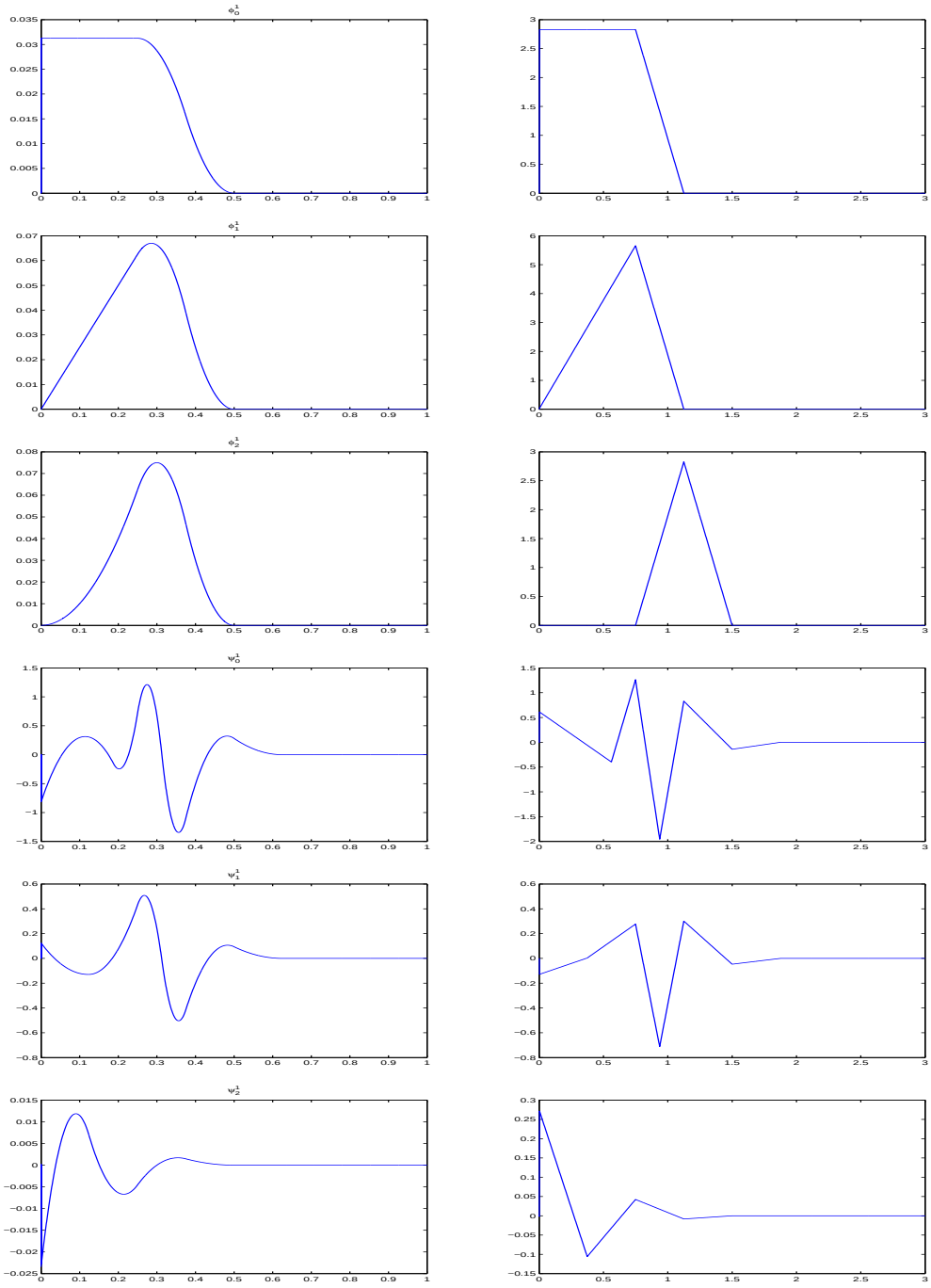

Figure 1: Left column: scaling functions $\Phi_\ell^{1,\flat}$ (three first rows) and wavelets $\Psi_\ell^{1,\flat}$ (three last rows). Right column: scaling functions $\Phi_\ell^{0,\flat}$ (three first rows) and wavelets $\Psi_\ell^{0,\flat}$ (three last rows) : B-Spline generators with $r = \tilde{r} = 3$.

.

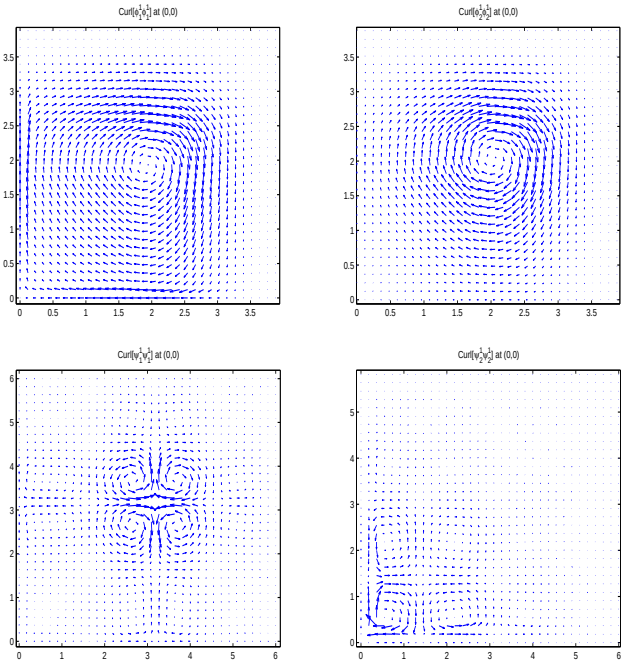

Figure 2: Vector field of divergence-free scaling functions $\mathbf{curl}[\Phi_1^{1,\flat} \otimes \Phi_1^{1,\flat}]$ and $\mathbf{curl}[\Phi_2^{1,\flat} \otimes \Phi_2^{1,\flat}]$, constructed from edge scaling functions: $\ell = 1,\ 2$ (first line), Vector field of divergence-free wavelets $\mathbf{curl}[\Psi_1^{1,\flat} \otimes \Psi_1^{1,\flat}]$ and $\mathbf{curl}[\Psi_2^{1,\flat} \otimes \Psi_2^{1,\flat}]$, constructed from edge wavelets: $\ell = 1,\ 2$ (second line).

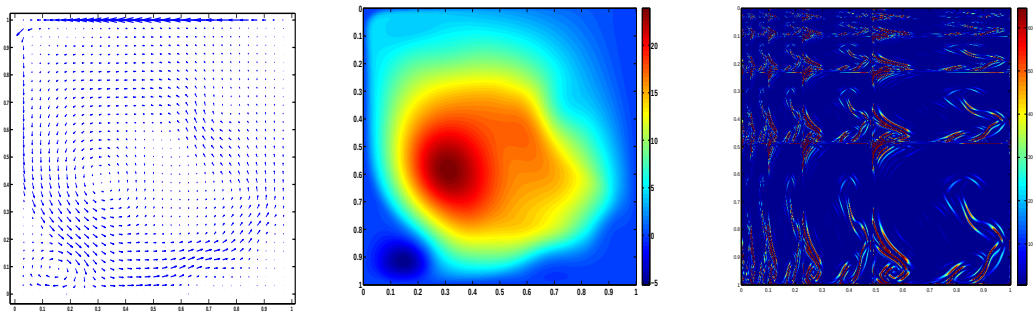

Figure 3: Example of vector field 512x512 (left), its divergence-free scaling function coefficients (middle) and renormalized divergence-free wavelet coefficients (right).

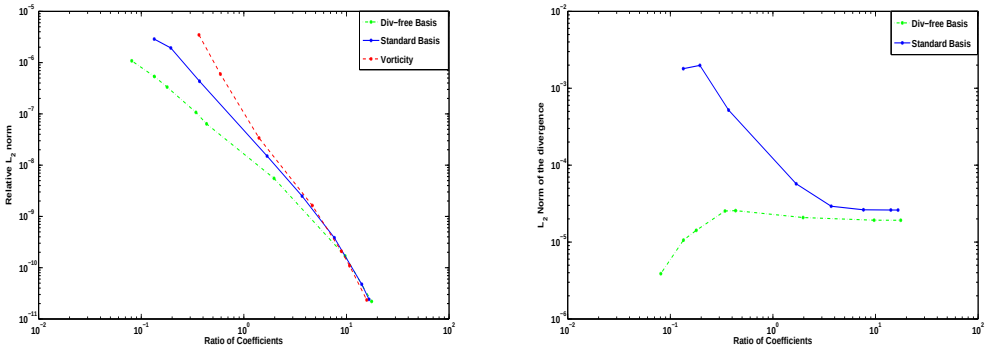

Figure 4: Left: relative nonlinear error versus the number of retained coefficients (in %):, computed on the velocity field of Figure 3, provided by divergence-free wavelets (green curve) and standard wavelets (blue), and the same for the vorticity in standard wavelets (red). Right: divergence of the N-best terms approximation of $\mathbf{u}$ in divergence-free wavelet approximation (green), and in standard vector wavelet approximation (blue).